Diagrammatic representation of interference colours in the presence of dispersion of birefringence

Florian Dufey

Diagrammatic representation of interference colours in the presence of dispersion of birefringence

Florian Dufey *

Feldstr. 18, 85716 Unterschleißheim, Germany

December 21, 2021

Abstract

Based on simulations similar to the ones used to generate high-quality Michel–Lévy charts, graphical representations of anomalous interference colours which are based on a linear model for the dispersion of birefringence are shown. In the charts, the path length difference $\Delta\Gamma_\mathrm{D}$ forms the ordinate, while the birefringence $\Delta\Gamma_\mathrm{F} - \Delta\Gamma_\mathrm{C}$ forms the abscissa. Using these charts, many facts which are in principle well known, but whose justification requires rather abstract argumentation, can be grasped intuitively. The usefulness is shown by comparison with several photographs of anomalous interference colours observed either on wedges or conoscopically on various minerals and substances spanning the whole range of possible linear dispersion ranges quantified by different Ehringhaus numbers N.

These diagrams may be of high pedagogical value in the teaching of polarisation microscopy and may complement the well known Michel–Lévy chart.

1 Introduction

It is well known that the index of refraction n is in general a function of the wavelength λ, $n = n(\lambda)$, which is known as dispersion of the index. With the exception of regions where substances show strong absorption, $n(\lambda)$ decreases with increasing wavelength. In anisotropic materials, the index of refraction depends on the orientation of the polarisation vector relative to the crystal. The change of n with λ is usually different for different directions of the polarisation too, so that also birefringence, $\Delta n(\lambda)$, becomes wavelength dependent, which is known as dispersion of the birefringence (DoB). This effect was first described by Herschel and Brewster (Herschel, 1820). By the end of the 19$^{\mathrm{th}}$ century, DoB was well understood (Hlawatsch, 1902, 1904) and its usefulness for mineral identification in polarisation microscopy came into focus. E.g., Ehringhaus (1920) tabulated measured DoBs for a number of minerals and substances.

While it is relatively easy for a student to get an intuitive understanding how to interpret normal interference colours using a Michel–Lévy chart, the description of the DoB in textbooks (Raith, Raase, and Reinhardt, 2012, Schumann and Kornder, 1973, Pichler and Schmitt-Riegraf, 1997) is often rather brief and may appear cryptic to the student.

With modern computer graphics it easy to calculate highly realistic Michel–Lévy charts as shown by Sørensen (2013). It is the aim of the present article, to extend this methodology to visualize the DoB and compare it to images of the DoB as observed on actual minerals and substances.

While there are minerals for which the dependence of DoB on wavelength is complicated, for the vast majority of them, it seems sufficient to assume this dependence to be rather smooth and simple so that it

*florian@dufey.net

can be described well by a first order Taylor expansion, e.g., in $1/\lambda^2$ (Cauchy dispersion) (Fig. 1), or directly in λ (Fig. 2). The difference between different first order approximations will be the smaller the narrower the wavelength range into question, which is quite restricted in the case of human vision, anyhow. It will be shown that in the linear approximation the interference colours show some periodicity which has early been observed and even been used to name some variety of apophyllite as leucocyclite, due to the periodic repetition of black and white interference colours with changing thickness. Due to this higher symmetry of the interference patterns, the linear approximation will be used in the generation of DoB charts.

After giving a discussion of the new graphical representation, its interpretation and some details of their generation, the simulation will be compared to photographs of interference patterns recorded either on wedge-shaped samples or conoscopically on slabs of several minerals and substances showing different degrees of DoB.

2 Dispersion of Birefringence

When trying to quantify DoB, birefringence is usually reported at the wavelengths of the three Fraunhofer lines C, D, and F, with $\lambda_\mathrm{D} = 589$ nm (yellow-orange), $\lambda_\mathrm{C} = 656$ nm (red), and $\lambda_\mathrm{F} = 486$ nm (sky blue). Just like the birefringence itself depends on the direction of the light ray relative to the main axes of the crystal, also DoB is orientation dependent. In uniaxial crystals, one usually reports the DoB measured for maximal birefringence. In crystals of lower symmetry, DoB is not as useful diagnostically, it may even change sign for different orientations of the crystal. Furthermore, in crystals from the tri- or monoclinic system, also the orientation of the principal axes of the crystal is in general wavelength dependent (dispersion of the axes). Notwithstanding sporadic works which tried to establish quantitative DoB measurements diagnostically (e.g. Hörmann and Raith (1971)), nowadays, the qualitative aspects of DoB are considered of most diagnostic value. Nevertheless, it is important to know how it can be quantified. Ehringhaus (1920) recommended to use the quotient

$$N = \frac{\Delta\Gamma_\mathrm{D}}{\Delta\Gamma_\mathrm{F} - \Delta\Gamma_\mathrm{C}} = \frac{\Delta n_\mathrm{D}}{\Delta n_\mathrm{F} - \Delta n_\mathrm{C}},$$

which is commonly referred to as the Ehringhaus number, to quantify the inverse of birefringence, where $\Delta\Gamma = d\Delta n$, with d being the thickness of the crystal. He also composed comprehensive tabulation of measured N for a large number of minerals and substances. For convenience (and with some corrections), this tabulation is available in the supplementary materials. If nothing else is said, N refers to an orientation of the crystal for which also the maximal value of Δn_D is observed. The Ehringhaus number has the advantage to be independent of the thickness of the crystal. For substances showing a $|N| > 30$, effects of DoB are to weak to be detected by the naked eye. E.g., $N = 33.7$ for quartz and $N = 23$ for calcite. Hence when using calcite compensators to measure DoB of other samples, its own DoB has to be taken into account.

If the birefringence in the blue Δn_F is greater than the birefringence in the red part of the spectrum, Δn_C, the resulting interference colours are called "supra-normal", while if $\Delta n_\mathrm{F} < \Delta n_\mathrm{C}$, one speaks of "sub-normal" interference colours. If Δn is zero for some λ in the visible range (from $\lambda_\mathrm{min} = 380$ nm to $\lambda_\mathrm{max} = 780$ nm), but dispersion is non-zero, the resulting interference colours are called "anomalous" in sensu stricto. In the linear approximation assumed, anomalous colors appear in the wedges with

$$N \leq \frac{\lambda_\mathrm{max} - \lambda_\mathrm{D}}{\lambda_\mathrm{C} - \lambda_\mathrm{F}} = 1.12$$

and

$$N \geq \frac{\lambda_\mathrm{min} - \lambda_\mathrm{D}}{\lambda_\mathrm{C} - \lambda_\mathrm{F}} = -1.23.$$

For Cauchy dispersion, slightly different values result, but it should be clear that this are not hard boundaries with a quantitative significance.

In the following diagram, the parameter N corresponds to lines of constant slopes through the origin. The corresponding colours lying on such a line will be observed on a wedge-shaped crystal (Fig. 4).

The assumption that the change of birefringence with wavelength is linear, means that

$$\Delta n(\lambda) \approx \Delta n_{\mathrm{D}} + \frac{d\Delta n}{d\lambda}(\lambda - \lambda_{\mathrm{D}}).$$

Within the same approximation, the differential quotient may be replaced by a quotient of differences

$$\Delta n(\lambda) \approx \Delta n_{\mathrm{D}} - \frac{\Delta n_{\mathrm{F}} - \Delta n_{\mathrm{C}}}{\lambda_{\mathrm{C}} - \lambda_{\mathrm{F}}}(\lambda - \lambda_{\mathrm{D}}). \qquad (1)$$

The difference $\Delta\Gamma_{\mathrm{F}} - \Delta\Gamma_{\mathrm{C}}$ is conveniently printed along the abscissa, while the ordinate values are taken as $\Delta\Gamma_{\mathrm{D}}$. When the $\Delta\Gamma$'s are measured in units of 25 μm, the values coincide numerically with the corresponding Δn for the standard thickness of thin sections. As the colours depend only on the relative sign of birefringence and its dispersion, it is sufficient to plot only positive values of birefringence.

In the resulting diagram (Fig. 2), besides the lines with $N = \pm 30$, which bound the region of normal interference colours, and the boundaries of the wedges below which anomalous colour in sensu stricto are observed. The line with slope $N = \lambda_{\mathrm{D}}/(\lambda_{\mathrm{F}} - \lambda_{\mathrm{C}}) = -3.46$ is shown, too. Along this line, $\Delta\Gamma(\lambda)$ is directly proportional to λ so that only black and white interference stripes are observed, but no colours. The apophyllite variant leucocyclite owes its name to this succession of black and white interference colors. This represents a special case of sub-normal interference colours. For a slab of such a material with $N = -3.46$, the optical path length difference $\Delta\Gamma$ is constant for all wavelengths, making it a perfect material for achromatic retardation plates. Below this line, also the ordering of the colours near an intensity minimum will be reversed.

The limits of the interference orders are defined as the values where the optical path difference is a multiple of the wavelength 551 nm (this value is somewhat arbitrary, sometimes 530 nm is used, instead). To extend these limits to materials with DoB, it seems reasonable to linearly extend them to pass through the intensity minima along the leucocyclite line.

While in the case of normal interference colours, the same interference colours are observed on a wedge-shaped crystal on one hand side and on a crystal of fixed thickness in combination with a compensator on the other hand side, this is no longer true for crystals showing DoB.

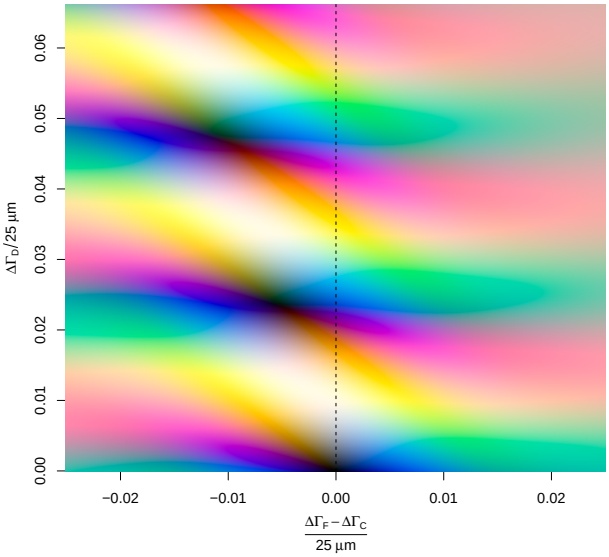

Figure 1: Plot of the anomalous interference colours as a function of $\Delta\Gamma_{\mathrm{F}} - \Delta\Gamma_{\mathrm{C}}$ and $\Delta\Gamma_{\mathrm{D}}$ assuming a Cauchy DoB and a light source emitting a blackbody radiation of temperature $T = 5100$ K.

3 Simulation of the anomalous interference colours

The simulation of the anomalous interference colours follows closely the methodology described by Sørensen (2013) to which the reader is referred for further details. The following information is needed:

1. The spectral intensity distribnution of the light source. In the examples shown below, a Planck curve describing the emission of a black body at 5100 K was used to model the spectrum of the halogen incandescent light source with daylight filter.

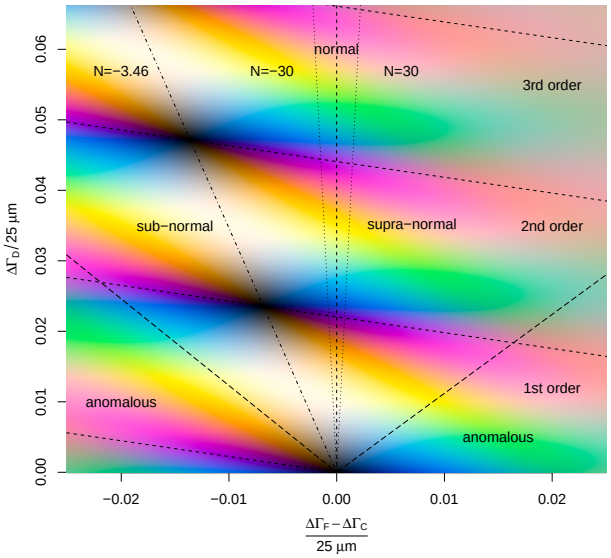

Figure 2: Plot of the anomalous interference colours as a function of $\Delta\Gamma_\mathrm{F} - \Delta\Gamma_\mathrm{C}$ and $\Delta\Gamma_\mathrm{D}$ assuming a linear DoB and a light source emitting blackbody ratiation of temperature $T = 5100$ K. To the right of the dashed line, colours are supra-normal and to the left sub-normal, respectively. The dotted lines of slope $N = \pm 30$ bound the range of colours perceived as normal. The dash-dotted line of slope $N = -3.46$ corresponds to special case of sub-normal colours, where only black and white colours appear. Along the direction of this line, the whole plot is periodic, which makes the concept of interference order more precise; the only slightly inclined dashed lines separate the different orders. Below the two long dashed lines anomalous colours in the strict sense can be found which arise when the birefringence changes sign inside the optical range.

2. The tristimulus functions describing the spectral sensitivity of the eye of a standard observer, as derived by the CIE (Smith and Guild, 1932).

3. The transmission $T(\lambda)$ of the polariser–crystal sandwich (polarisers crossed),

$$T(\lambda) = \frac{1}{2}\left(1 - \cos\left(\frac{2\pi d \Delta n(\lambda)}{\lambda}\right)\right),$$

where $\Delta n(\lambda)$ is given by eq. 1.

Only the latter expression is more general than the one used in Sørensen (2013) whence it shall be discussed in more detail: Using eq. 1, one obtains

$$T(\lambda) = \frac{1}{2}\Bigg(1 - \cos\Bigg(\frac{2\pi d}{\lambda}\left(\Delta n_\mathrm{D} + \lambda_\mathrm{D}\frac{\Delta n_\mathrm{F} - \Delta n_\mathrm{C}}{\lambda_\mathrm{C} - \lambda_\mathrm{F}}\right) - \\ - 2\pi d \frac{\Delta n_\mathrm{F} - \Delta n_\mathrm{C}}{\lambda_\mathrm{C} - \lambda_\mathrm{F}}\Bigg)\Bigg). \quad (2)$$

Clearly, the term in the second line corresponds to a constant phase shift induced by DoB. As the cosine is periodic, from the observation of DoB at a given thickness of the crystal slab, this phase, and hence also the DoB can only be estimated up to a multiple of 2π. This also explains the periodicity of the interference colour pattern. Thus for thick slabs, it becomes difficult to estimate the interference order. Specifically, a slab with a thickness d such that the quantity

$$d\frac{\Delta n_\mathrm{F} - \Delta n_\mathrm{C}}{\lambda_\mathrm{C} - \lambda_\mathrm{F}}$$

is integer will show the same interference colours with a compensator as a mineral without DoB (that is, the usual colours form the Michel–Lévy chart). However, the point of complete extinction will no longer correspond to the zeroth interference order. If this quantity is half integer, the interference colours will be those observed on a mineral without DoB with parallel polariser and analyser direction, as rotation of the analyzer by $\theta = \pi/2$ corresponds to an overall phase shift of $2\theta = \pi$.

4 Examples

Experimentally obtained interference patterns were recorded for several minerals or chemical substances. All photographs where taken on a Leitz Orthoplan Pol microscope, using an incandescent halogen illumination with a daylight filter whose spectral distribution was modelled by a Planck curve of colour

temperature $T = 5100$ K. To record the variation of birefringence with path length d, in the first example, a wedge shaped sample was used. For the other substances, suitable wedges were not available. Instead, conoscopic figures obtained for planar slabs of uniaxial substances cut perpendicular to the optical axis were were recorded using a Bertrand lens. In these conoscopic figures, both path length and birefringence increases monotonically with the radial distance from the center, whence the sequence of the colours of the isochromates is identical to the ones one would observe on a wedge in orthoscopic mode. Of course, the spacing of the isochromates differs from the colour spacing observed on a wedge. As the radial distance of the isochromates depends on other factors, like the mean index of refraction of the sample in question, it was not intended to simulate this dependence. Rather, in all the simulations the the colour pattern which would result for a wedge is shown. In Fig. 3, the same interference colours as in Fig. 2 are shown, but in addition lines of slope N corresponding to the Ehringhaus numbers of the samples analyzed are printed. As the Ehringhaus numbers of the samples were not available, these numbers where optimized manually so as to produce an optimal visual similarity of the observed colours and the simulated ones. Where available, values tabulated in the work of Ehringhaus (1920) are reported for comparison.

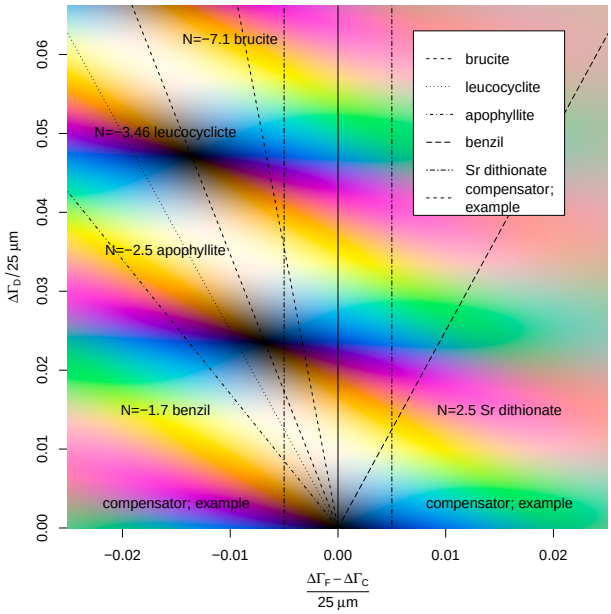

Figure 3: Plot of the anomalous interference colours as a function of $\Delta\Gamma_F - \Delta\Gamma_C$ and $\Delta\Gamma_D$ assuming a blackbody source of temperature $T = 5100$ K. Also shown are the simulated interference colours for several substances. The line with $N = -2.5$ belongs to an apophyllite with very sub-normal colours so that the order of the interference colours is even inverted. The line with $N = -3.46$ belongs to another apophyllite named leucocyclite, which nearly shows a periodic black and white pattern. The line with $N = -1.7$ belongs to the organic compound benzil. The line with $N = 3$ belongs to strontium dithionate tetrahydrate, and shows very supra-normal colours. As an example, also the vertical lines along which birefringence varies for a fixed value of dispersion $= 0.005$ are shown, as would be observed with a compensator.

4.1 Apophyllite

The first example Fig. 4, shows the interference pattern for a wedge made from apophyllite. Interference order increases with thickness from left to right. The simulated spectrum, assuming $N = -2.5$ coincides very well with the recorded one. The small shift of the left side of the recorded spectrum and the measured one takes account of the fact, that wedges cannot be made infinitely thin. The N of different samples of apophyllite are very variable. Ehringhaus lists values of 0.63, -0.065, -1.5, -1.9, and -5.6. In the interference pattern it strikes the eye that the order of the interference colours is reversed when compared to normal dispersion. It can be seen that this is the case for all N between -3.46 and 0. Ehringhaus proposed to call this DoB range "anti-normal".

4.2 Brucite

The next example is the mineral brucite, Fig. 5. The picture is taken in conoscopic mode, so that the distance of the isochromates does not correspond to the distances of the colours in the simulation. Ehringhaus reports a value of $N = -7.1$ and this seems to describe the interference pattern very well. The or-

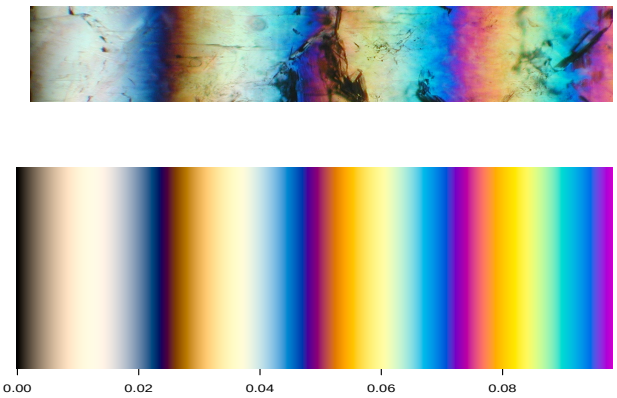

Figure 4: Interference colours of a wedge of apophyllite. Its sub-normal interference pattern is reproduced well by a simulation with $N = -2.5$ (see insert).

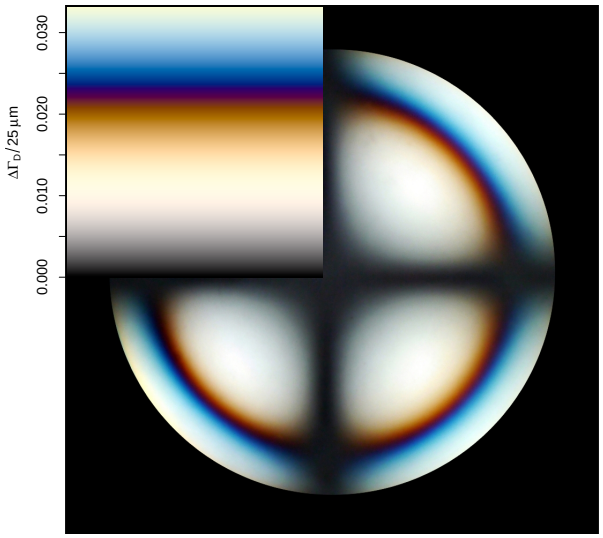

Figure 5: Interference colours on consoscopic observation (isochromates) of brucite. Its sub-normal interference colours are reproduced well by a simulation with $N = -7.1$ (see insert).

der of the interference colours is still normal, but the hue is darker.

4.3 Leucocyclite

Leucocyclite, here also shown in conoscopic mode, is a variant of apophyllite whith a value of N near -3.46. If the dispersion were really linear with this Ehringhaus number, the interference orders would be a succession of black and white light. Even small deviations both from linearity and in N are therefore visible in the form of coloured fringes on both sides of the minima.

4.4 Benzil

Benzil (1,2-diphenylethane-1,2-dione) is an organic compound and has the smallest value of $N = -1.7$ among the examples shown. The colours are of comparable intensity as normal interference colours, albeit their order is reversed. The coincidence of the observed and simulated colours is striking. Benzil crystallizes in the rhombohedric enantiomorphic crystal structure $P3_121$, (More, Odou, and Lefebvre, 1987), although the benzil molecule is achiral. This explains the brightening of the center of the conoscopic figure.

4.5 Strontium dithionate tetrahydrate

The last example is the DoB of the substance strontium dithionate tetrahydrate, $Sr_2S_2O_6 \cdot 4H_2O$, which shows supra-normal colours with $N = 2.4$ (Ehringhaus reports an even smaller value $N = 1.8$). The first order colours are very intense and in the same order as in substances without DoB, but already the second order appears faded as colours of high normal order.

5 Discussion

Polarisation microscopy is still an essential tool in geo-science as, in contrast to more advanced meth-

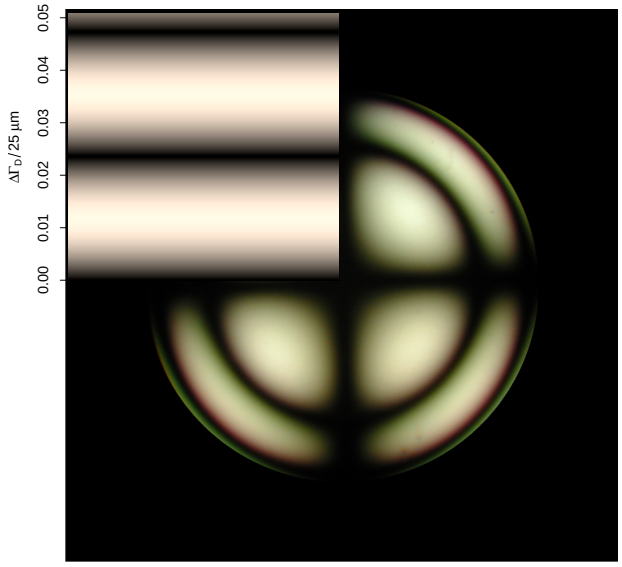

Figure 6: Conoscopic figure of the apophyllite variety leucocyclite. Its sub-normal black and white interference pattern is reproduced well by a simulation with $N = -3.46$ (see insert).

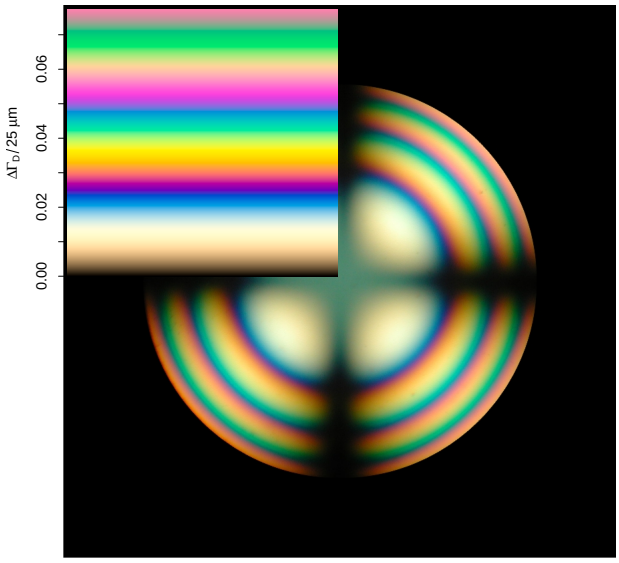

Figure 7: Conoscopic figure of the organic compound benzil. Its sub-normal interference pattern is reproduced well by a simulation with $N = -1.7$ (see insert).

ods, it yields an overview of the mineral content and structure of a thin section. However, to be able to extract the wealth of information which can be obtained by microscopic analysis, considerable training effort by the student is required. Graphical charts, like the Michel–Lévy chart of interference colours, are invaluable pedagogical tools which also induce new questions like why we observe different interference orders whose colour sequence is similar but gets more faint with increasing order. The answer becomes intuitively clear from a look at Fig. 2, where strict periodicity pertains along the direction with slope $N = -3.46$, which is realized to good approximation in minerals like leucocyclite. This periodicity does not disappear when going away from this line to the region of normal birefringence, but for higher orders, these will overlap increasingly and therefore the orders become more faint. While this relation is immediately obvious looking at the figure, even an expert like Ehringhaus, who dedicated his thesis to the study of DoB, was truly astonished to be able to distinguish more than 36 interference orders on a wedge of leucocyclite while, from his experience with wedges of quartz, he would have expected no more than 20. It can also be seen that interference orders will wash out even more rapidly for small (positive and negative) values of N, which coincides with the observations on conoscopic figures of benzil or strontium dithionate.

Another point which becomes intuitively clear is the inversion of the order in which interference colours appear for values of $N < -3.46$ (cf. the benzil example).

It becomes also apparent that the anomalous colours in sensu stricto are not special. The dark blue, violet or brownish colours observed on minerals like melilite or chlorite are often mistaken by the student for first order colours. From the Figs. 2, 4 or 5 it can be seen that the first order colours of apophyllite or brucite, which show sub-normal interference

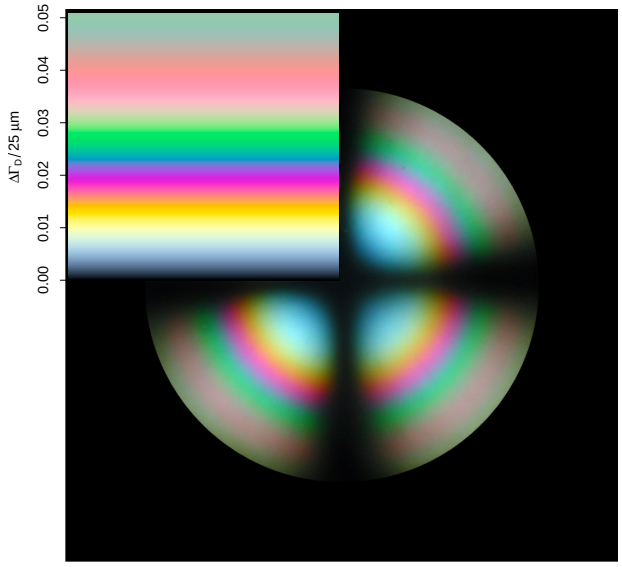

Figure 8: Conoscopic figure of Strontium dithionate tetrahydrate. Its supra-normal interference pattern is reproduced well by a simulation with $N \approx 2.5$ (see insert).

colours near the leucocyclite line, are very similar to anomalous colour in sensu stricto.

This leads naturally to the explanation of another observation, namely the incompensatability of DoB. From diagrams 2 and 3, it can be inferred that upon changing the thickness of a mineral slab, one moves along the lines of constant slope N. Compensators are typically made from materials like calcite or MgF_2, which show only negligible DoB and for which the corresponding lines are almost vertical. While changing thickness d of a single slab or wedge yields lines passing through the origin, the situation becomes more complicated for a combination of two materials, one of them being the compensator. In Fig. 3 two dash dotted vertical lines are shown to exemplify the effect of an idealized compensator. In its zero position, one would for example observe yellow colours on a slab of strontium dithionate where the line with $N = 2.5$ and the vertical compensator line cross. If now $\Delta\Gamma_D$ is compensated, instead of the expected black, anomalous, deep blue colours would be observed. This is known as incompensability of DoB. If the compensator is now moved further, due to the restricted range and symmetry of the graphic, the vertical line has to be continued on the left side of the graphic at negative abscissa values. Upon further compensation, one passes first through white and then through nearly black colours at abscissa values of $\Delta n_D \sim 0.024$. With only the Michel–Lévy chart in mind, one would erroneously conclude that this point represents the true compensation point. In fact, in the presence of DoB, with only a compensator it becomes impossible to determine the interference order, especially if the slab is either very thick or DoB is strong.

A final point concerns the variation of strictly anomalous interference colours with composition as observed for example in melilite crystals. In these crystals, the composition sometimes changes between one with higher åkermanite fraction in the center and one with higher gehlenite content in the fringes. If the molar fraction of gehlenite is x, the birefringence can be developed into a Taylor series in both x and λ to first order,

$$\Delta n(x,\lambda) \approx \left.\frac{\partial \Delta n}{\partial x}\right|_{x_0,\lambda_D} (x - x_0) + \left.\frac{\partial \Delta n}{\partial \lambda}\right|_{x_0,\lambda_D} (\lambda - \lambda_D),$$

where x_0 is the molar fraction of the average composition. The difference $\Delta n_F - \Delta n_C$ plotted on the abscissa, is therefore independent of composition in this approximation, while the ordinate values Δn_D are proportional to $x - x_0$. Hence the variation of the interference colours one observes with changing composition will follow the same compensator lines as shown in Fig. 3 for small values of Δn_D, cf. Raith et al. (2012, Fig. 4-36, p. 98), which also means that this colour change can be simulated with a compensator.

Many materials, for which the determination of the DoB might be useful, like e.g. Chlorites, show some absorption colours. However, as nowadays it is easy to attach a digital camera to any microscope (even smart phones cameras yielding excellent pictures), it is possible to first take a picture with the analyzer removed, and use this picture to perform

white-balancing on the picture taken with crossed polarizers. The corrected picture will then ideally show cthe pure colours due to birefringence, only.

In conclusion, a diagram like Fig. 2, despite the underlying idealizations, appears to be a potentially very valuable tool in the teaching of the use of the polarizing microscope and can complement the well established Michel–Lévy chart.

Acknowledgement

I am deeply indebted to Olaf Medenbach for providing the photographs shown in the text.

References

Ehringhaus, A.: Über Dispersion der Doppelbrechung bei Kristallen, Neues Jahrbuch für Mineralogie, Geologie und Paläontologie, 43, 557–618, 1920.

Herschel, J. F. W.: IV. On the action of crystallized bodies on homogeneous light, and on the causes of the deviation from Newton's scale in the tints which many of them develope on exposure to a polarised ray, Philosophical Transactions of the Royal Society of London, pp. 45–100, 1820.

Hlawatsch, C.: IX. Bestimmung der Doppelbrechung für verschiedene Farben an einigen Mineralien., Tschermaks mineralogische und petrographische Mitteilungen, 21, 107–158, 1902.

Hlawatsch, C.: XXVI. Bestimmung der Doppelbrechung für verschiedene Farben an einigen Mineralien., Tschermaks mineralogische und petrographische Mitteilungen, 23, 415–450, 1904.

Hörmann, P. and Raith, M.: Optische Daten, Gitterkonstanten, Dichte und magnetische Suszeptibilität von Al-Fe (III)-Epidoten, N Jahrb Mineral Abh, 116, 41–60, 1971.

More, M., Odou, G., and Lefebvre, J.: Structure determination of benzil in its two phases, Acta Crystallographica Section B: Structural Science, 43, 398–405, 1987.

Pichler, H. and Schmitt-Riegraf, C.: Rock-forming minerals in thin section, Springer, Heidelberg, second edn., doi:10.1007/978-94-009-1443-8, 1997.

Raith, M. M., Raase, P., and Reinhardt, J.: Guide to Thin Section Microscopy, second edn., URL `http://www.minsocam.org/msa/openaccess_publications/thin_sctn_mcrscpy_2_rdcd_eng.pdf`, 2012.

Schumann, H. and Kornder, F.: Rinne/Berek, Anleitung zu optischen Untersuchungen mit dem Polarisationsmikroskop, Schweizerbart'sche Verlagsbuchhandlung, Stuttgart, third edn., 1973.

Smith, T. and Guild, J.: The CIE colorimetric standards and their use, Transactions of the optical society, 33, 75–134, 1932.

Sørensen, B.: A revised Michel–Lévy interference colour chart based on first-principles calculations, European Journal of Mineralogy, 25, 5–10, doi: 10.1127/0935-1221/2013/0025-2252, 2013.